



# MazF activation causes ACA sequence-independent and selective alterations in RNA levels in *Escherichia coli*

Kentaro Akiyama<sup>1</sup> · Kazuki Fujisawa<sup>1</sup> · Hiro Kondo<sup>1</sup> · Yuya Netsu<sup>1</sup> · Koji Nishikawa<sup>1</sup> · Yoshio Takata<sup>1</sup> · Yuya Nakamura<sup>2</sup> · Yuta Kino<sup>2</sup> · Shotaro Ayukawa<sup>3</sup> · Masayuki Yamamura<sup>4</sup> · Nobuhiro Hayashi<sup>2</sup> · Yoh-ichi Tagawa<sup>2</sup> · Nobutaka Nakashima<sup>3,2,5</sup>

Received: 7 June 2019 / Revised: 21 August 2019 / Accepted: 27 August 2019 / Published online: 4 September 2019  
© Springer-Verlag GmbH Germany, part of Springer Nature 2019

## Abstract

*Escherichia coli* MazF is a toxin protein that cleaves RNA at ACA sequences. Its activation has been thought to cause growth inhibition, primarily through indiscriminate cleavage of RNA. To investigate responses following MazF activation, transcriptomic profiles of *mazF*-overexpressing and non-overexpressing *E. coli* K12 cells were compared. Analyses of differentially expressed genes demonstrated that the presence and the number of ACA trimers in RNA was unrelated to cellular RNA levels. Mapping differentially expressed genes onto the chromosome identified two chromosomal segments in which upregulated genes formed clusters, and these segments were absent in the chromosomes of *E. coli* strains other than K12. These results suggest that MazF regulates selective, rather than indiscriminate, categories of genes, and is involved in the regulation of horizontally acquired genes. We conclude that the primary role of MazF is not only cleaving RNA indiscriminately but also generating a specific cellular state.

**Keywords** Horizontal gene transfer · MazF · Metatranscriptome · RNA-interferase · RNA-seq · Toxin-antitoxin

---

Communicated by Erko Stackebrandt.

---

**Electronic supplementary material** The online version of this article (<https://doi.org/10.1007/s00203-019-01726-9>) contains supplementary material, which is available to authorized users.

---

✉ Nobutaka Nakashima  
n-nakashima@aist.go.jp

- <sup>1</sup> iGEM Team Tokyo\_Tech 2016, Tokyo Institute of Technology, 2-12-1 Ookayama, Meguro-ku, Tokyo 152-8550, Japan
- <sup>2</sup> School of Life Science and Technology, Tokyo Institute of Technology, 2-12-1 Ookayama, Meguro-ku, Tokyo 152-8550, Japan
- <sup>3</sup> Bioproduction Research Institute, National Institute of Advanced Industrial Science and Technology (AIST), 2-17-2-1 Tsukisamu-Higashi 2-jyo, Toyohira-ku, Sapporo 062-8517, Japan
- <sup>4</sup> School of Computing, Tokyo Institute of Technology, 4259 Nagatsuta-cho, Midori-ku, Yokohama 226-8503, Japan
- <sup>5</sup> Computational Bio Big Data Open Innovation Laboratory (CBBD-OIL), AIST, 2-17-2-1 Tsukisamu-Higashi, Toyohira-ku, Sapporo 062-8517, Japan

## Introduction

Bacterial chromosomes encode various toxin–antitoxin (TA) systems. For example, the chromosome of the *Escherichia coli* MG1655 strain, a derivative of the K12 lineage, encodes at least 37 TA systems (Yamaguchi and Inouye 2011; Wang et al. 2012). The function of a toxin-encoding gene is repressed by the action of a cognate antitoxin gene in vegetatively growing cells but is de-repressed (activated) under certain conditions to cause complete cell death, reversible growth arrest, or both (Van Melderen and Saavedra De Bast 2009; Tripathi et al. 2014).

TA systems are classified into six types (type I–type VI) according to their mode of action (Aakre et al. 2013; Masuda et al. 2012; Yamaguchi and Inouye 2011; Wang et al. 2012). In type II TA systems, which have been studied the most, toxin proteins cause dysfunction in essential cellular processes, and cognate antitoxin proteins repress the actions of toxins through direct protein–protein interactions. Under conditions of stress, antitoxins of type II TA systems are degraded by stress-induced proteases, and consequently toxins are activated. *mazEF* is one of the most widely distributed type II TA systems in bacteria. The *E. coli mazF* gene

encodes a toxin that is an ACA-specific endoribonuclease (RNA interferase). MazF activation has been thought to cause growth inhibition through indiscriminate cleavage of RNA, because 96% of *E. coli* coding sequences have at least one ACA sequence (Venturelli et al. 2017).

However, how growth inhibition is evoked following MazF activation remains unclear at the molecular level. To address this issue, omics analyses of *mazF*-overexpressing cells have been carried out. Typical RNA-seq and Poly-seq (polysome fractionation coupled with RNA-seq) analyses revealed that the activation of MazF leads to a reduction in the translation of the genes involved in cell metabolism and energy supply, as well as the selective synthesis of the "MazF-regulon" proteins (Sauert et al. 2016). In contrast, other transcriptome and proteome analyses indicated the non-selective synthesis of MazF-regulon proteins but the overall inhibition of protein synthesis after MazF activation (Culviner and Laub 2018; Mets et al. 2019). Time-series RNA-seq measurements of MazF-induced cells (2–8 min) showed the inhibition of cell division and specific upregulation of 11 TCA cycle enzymes (Venturelli et al. 2017). However, we assume that these studies lacked satisfactory biological replicates and/or bioinformatic analysis. In this study, we compared the transcriptomic profile of *mazF*-overexpressing cells to that of control non-expressing cells based on three biological replicates. From the results, many differentially expressed genes (DEGs) were detected, and bioinformatic analyses of DEGs highlighted new biological roles for MazEF.

## Materials and methods

### *E. coli* strains and general techniques

Wild-type *E. coli* K12 MG1655 (obtained from the National Bio Resource Research Project: NBRP, NIG, Japan) was used as the host strain. Cells were cultured in Luria broth in the presence or absence of appropriate antibiotics at 37 °C, unless otherwise stated. When expressing *mazF* from plasmids, transformants were pre-grown overnight, diluted 1:400 with fresh Luria broth, and cultured for 1.7 h. Next, L-arabinose was added to the medium at a final concentration of 0.1% to induce gene expression from plasmids.

### Plasmid construction

To construct pBAD-mazF, a double-stranded DNA fragment containing the ribosomal-binding sequence (RBS) was prepared by hybridizing two complementary synthetic oligonucleotides (sGEM12, 5'-ctagagaagaggagaataactagtagcg-gccgctgca; sGEM13, 5'-gcgccgctactagtagtattctccttct). The hybridized fragment was cloned into the SpeI–PstI moiety

of pSB1C3-BAD (parts ID BBa\_I0500, iGEM Foundation, Cambridge, MA), yielding pBAD-RBS/C. The pBAD-RBS/C plasmid was treated with EcoRI and PstI, and the resulting fragment containing the RBS was cloned into the EcoRI–PstI moiety of pSB6A1 (iGEM foundation), yielding pBAD-RBS. A DNA fragment containing the *mazF* coding sequence was PCR-amplified from MG1655 total DNA using a specific primer set (sGEM14, 5'-aaactagatggtaa-gccgatactaccgat and sGEM15, 5'-aaactgacggccgctactagtagtattaccgaatcagtagcttaattttggcttaagt). The fragment was treated with XbaI and PstI and cloned into the SpeI–PstI moiety of pBAD-RBS yielding pBAD-RBS-mazF/C. Then, the *mazF*-containing fragment was excised from pBAD-RBS-mazF/C using EcoRI and PstI and cloned into the EcoRI–PstI moiety of pSB6A1, yielding pBAD-mazF.

To construct plac-mazE, a DNA fragment containing lac promoter–RBS was excised from plac-RBS/C (parts ID BBa\_J04500, iGEM Foundation) using EcoRI and PstI and cloned into the EcoRI–PstI moiety of pSB3K3 (iGEM Foundation), yielding plac-RBS. A DNA fragment containing the *mazE* coding sequence was PCR-amplified from MG1655 total DNA using a specific primer set (sGEM16, 5'-aaactagatgatccacagtagcgtaaagcgttg and sGEM17, 5'-aaactgacgg-cgcgctactagtagtattaccagactccttattcttcggctctc). The fragment was treated with XbaI and PstI and cloned into the SpeI–PstI moiety of plac-RBS/C, yielding plac-RBS-mazE/C. Then, plac-RBS-mazE/C was treated with EcoRI and PstI and the resulting *mazE*-containing fragment was cloned into the EcoRI–PstI moiety of plac-RBS, yielding plac-mazE.

### RNA extraction and sequencing by next generation sequencing (RNA-seq)

Before harvesting, cells were treated with RNAprotect Bacteria Reagent (Qiagen, Valencia, CA) to stabilize RNA. Total RNA was extracted using the acid hot phenol method (Aiba et al. 1981) and purified using an RNeasy Mini Kit (Qiagen) according to the manufacturer's protocol. The MICROB-Express Bacterial mRNA Enrichment kit (Ambion, Austin, TX) was applied to total RNA to remove excess rRNA. cDNA libraries were constructed using a TruSeq Stranded mRNA and Total RNA Sample Preparation Kit (Illumina Inc., San Diego, CA) and sequenced with a MiSeq sequencer (Illumina) in paired-end-read mode for 2 × 75 cycles. Each sample was analyzed in triplicate. To obtain the read number, all samples were sequenced with MiSeq twice.

### Sequence analysis

High-quality RNA-seq reads were filtered using the trimomatic program version 0.36 (Bolger et al. 2014) with the following parameters: 'SE CROP:68 HEADCROP:7 MINLEN:18'. Reads were mapped to the chromosome by

the EDGE-pro program version 1.3.1 (Magoc et al. 2013) using default settings. The numbers of mapped reads were 3,676,809, 6,611,324, and 5,350,605 for experiments on control cells and 5,002,966, 5,112,654, and 5,354,611 for experiments using *mazF*-overexpressing cells. Transcriptome profiles were compared using the edgeR package of R (McCarthy et al. 2012) with the exactTest mode. The genome index, gene annotation, and genome-sequence files were downloaded from the RefSeq web site (MG1655 GCA\_000005845.2\_ASM584v2 version). The Biostrings package of R (Ellrott et al. 2002) was used to count the number of ACA trimers in individual genes from a multi-fasta formatted file of the chromosomal sequence. To visualize the circular chromosome, the cgview program was used (Stothard and Wishart 2005).

RNA-seq data has been deposited in DDBJ/ENA/GenBank under Bioproject number PRJDB5742 and BioSample number SAMD00079815–SAMD00079832.

## Results

### Identification of DEGs and the number of ACA trimers following *mazF* activation

To express *mazF* in an inducible manner, a plasmid harboring the L-arabinose-inducible *bad* promoter and the *mazF* gene was constructed (pBAD-*mazF*). As expected, growth of the transformant with pBAD-*mazF* was inhibited upon the addition of L-arabinose (Supplementary Fig. S1). Besides, this phenotype was rescued by the 20-min delayed induction of *mazE* from the plasmid plac-*mazE* (Supplementary Fig. S1).

To investigate the cellular response following *mazF* activation, transcriptome profiles were compared between

*mazF*-overexpressing and non-expressing cells. Cells harboring pBAD (an empty vector) or pBAD-*mazF* were cultured and treated with L-arabinose for 20 min, and RNA from these cells was subjected to RNA-seq analysis. When DEGs were defined as a log<sub>2</sub>-fold change > 2.5 and with false discovery rate (FDR) < 1.0 × 10<sup>-2</sup>, 266 and 245 genes were found to be up- and down-regulated, respectively, among 4318 genes (the full data set is shown in Supplementary Table S1). Relative levels of *mazF* mRNA increased by 54-fold with an FDR of 1.3 × 10<sup>-6</sup>.

For the first transcriptome analysis, the numbers of ACA trimers in each gene were enumerated for the total, upregulated, and down-regulated gene sets (Table 1). Assuming that MazF has an enhanced opportunity to cleave ACA-rich RNA, compared to that with ACA-less RNA and that the cleaved RNA is further rapidly degraded by RNases, ACA-less RNA, and short-length RNA would be enriched in the upregulated gene set. Likewise, opposite effect should be observed in down-regulated genes. However, no such enrichment was observed, and especially, RNA species with no ACA sequence were not enriched in the upregulated gene set. Therefore, RNA levels following MazF activation are not determined by the presence of ACA trimers. In contrast, a preceding study showed that the number of ACA trimers was negatively correlated with the mean log<sub>2</sub>-fold change in RNA abundance 8 min after the overexpression of MazF; however, such correlations were only observed for RNA species with fewer than three ACA trimers, and no correlations were observed after 2 min of overexpression (Venturelli et al. 2017). We then calculated the mean log<sub>2</sub>-fold change in RNA abundance and similarly investigated the correlation using our data (20-min overexpression), again showing no correlation (Supplementary Table S1). Altogether, the presence and

**Table 1** Comparison of the numbers of ACA trimers within coding sequences between *mazF*-overexpressing and non-expressing *E. coli* K12 MG1655 cells

	All genes	Upregulated genes	Down-regulated genes
Number of genes <sup>a</sup>	4318	266	245
Average number of ACA sequences in one gene	10.7	12.1	11.0
Average number of ACA sequences in one gene per 100 bp	3.41	3.66	3.94
Number of genes containing no ACA sequences <sup>b</sup>	175 (4.1%)	11 (4.1%)	6 (2.5%)
Number of genes containing one ACA sequences <sup>c</sup>	326 (7.6%)	15 (5.6%)	25 (10%)
Number of genes containing two ACA sequences <sup>d</sup>	408 (9.4%)	19 (7.1%)	29 (12%)
Number of genes containing greater than 30 ACA sequences <sup>e</sup>	135 (3.1%)	12 (4.5%)	9 (3.7%)
Average length of coding sequence (bp)	315	328	291

<sup>a</sup>These numbers were determined using only coding sequences

<sup>b–e</sup>The percentage in parenthesis indicates the ratio between the number of total genes and the number of genes containing no, one, two, or greater than 30 ACA sequences (b/a, c/a, d/a, or e/a % in each column)

number of ACA trimer determines RNA levels following MazF activation only under very specific conditions.

### Biased distribution of DEGs on the chromosome

When mapping DEGs onto the *E. coli* circular chromosome, we found an uneven distribution (Fig. 1). In the chromosomal segments of 200–440 (named segment I) and 4480–4600 (segment II) kbp, a cluster of upregulated genes was formed, and no down-regulated genes were included. We further noticed that these two segments coincided with the specific segments reported by Karcagi et al. (2016); they found the segments that were present in the *E. coli* K12 MG1655 strain but absent in five other *E. coli* strains and deleted genes in these segments to construct a genome-streamlining strain MDS69 (the reconstructed genome map is shown in Supplementary Fig. S2). It should be noted that these segments contained only nonessential genes for growth and were assumed to be DNA containing genes for toxins, virulence factors, and mobile genetic elements that were recently acquired by horizontal transmission (Karcagi et al. 2016). Although the chromosomal segments of 1390–1480 kbp (segment III) also included a cluster of deleted genes in the MDS69 strain (Supplementary Fig. S2), this segment did not contain a cluster of upregulated genes (Fig. 1).

Meanwhile, when growth-essential genes (302 genes) (Yamazaki et al. 2008) were mapped similarly, no or few

were found in segments I–III (Fig. 1; the reconstructed genome map is shown in Supplementary Fig. S3). Of 266 and 245 up- and down-regulated genes, two and 30 were growth-essential genes, respectively, and 88 and 26 genes were deleted genes in the MDS69 strain, respectively. Collectively, we conclude that MazF regulates gene expression non-uniformly. Clusters of strain-specific genes are upregulated, possibly reflecting involvement of MazF in the activation of horizontally acquired genes. In contrast, growth-essential genes tend to be down-regulated. To our knowledge, this is the first report to show that MazF-regulated genes form clusters in specific chromosomal segments.

### Categorization of DEGs according to function

For an overview, DEGs and all genes were categorized into functional groups according to the KEGG Orthology (KO) database (Table 2) (Kanehisa et al. 2012). The most remarkable change was observed for the energy metabolism category; only one gene in this category (0.78%) was upregulated, whereas 42 genes (33%) were down-regulated. Moreover, in the carbohydrate metabolism category, 23% of genes were down-regulated. These results suggest that cells affirmatively limit energy acquisition from carbohydrates after MazF activation, and consequently, growth inhibition might occur. Similar results have been obtained by others, which have revealed that the activation of MazF leads to the downregulation of process associated with metabolism and energy supply (Sauert et al. 2016).

### Enriched cellular pathways in DEGs

In the preceding section, DEGs were categorized into rough functional groups. To categorize DEGs and interpret the RNA-seq results in greater detail, gene ontology (GO) enrichment analysis was implemented using DAVID (Database for Annotation, Visualization and Integrated Discovery) with the default settings (Huang et al. 2009). From the resulting annotation list, the enriched cellular pathways (KEGG Pathways) were extracted, with a  $p$  value < 0.05 considered significant (Table 3). This analysis revealed that with respect to the upregulated genes (1) thiamine metabolism, (2) valine, leucine, and isoleucine biosynthesis, and (3) 2-oxocarboxylic acid metabolism pathways were enriched. The latter two pathways are closely related, and both are involved in branched chain amino acids biosynthesis. However, the biological role of this upregulation is unclear.

With respect to the downregulated genes, the result again suggests that cells are limited in acquiring energy from carbohydrate following MazF activation, and this limitation is accomplished at multiple metabolic pathways such as glycolysis, TCA cycle, oxidative phosphorylation, and sugar uptake (PTS) (Table 3). Besides, 11 genes

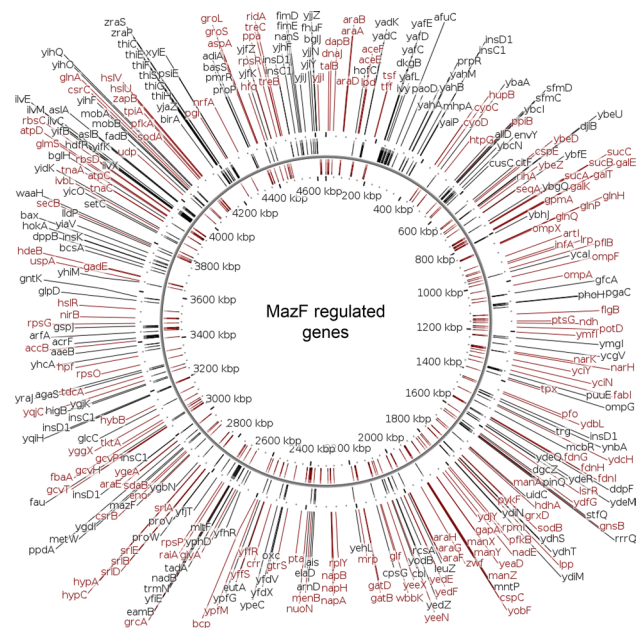


**Fig. 1** Chromosomal mapping of MazF-regulated genes in *E. coli* K12 MG1655. The black lines and characters indicate upregulated genes, and the brown lines and characters indicate downregulated genes. The full data set used for mapping is shown in Supplementary Table S2 (color figure online)

**Table 2** Functional categories of DEGs

KO categories	All genes <sup>a</sup>	Upregulated genes <sup>b</sup>	Downregulated genes <sup>c</sup>
Carbohydrate metabolism	469	21 (4.5%)	110 (23%)
Energy metabolism	128	1 (0.78%)	42 (33%)
Lipid metabolism	84	7 (8.3%)	3 (3.6%)
Nucleotide metabolism	150	4 (2.7%)	11 (7.3%)
Amino acid metabolism	271	19 (7.0%)	25 (9.2%)
Metabolism of other amino acids	80	2 (2.5%)	4 (5.0%)
Glycan biosynthesis and metabolism	57	0 (0%)	1 (1.8%)
Metabolism of cofactors and vitamins	163	12 (7.4%)	7 (4.3%)
Metabolism of terpenoids and polyketides	33	2 (6.1%)	0 (0%)
Biosynthesis of other secondary metabolites	25	0 (0%)	1 (4.0%)
Xenobiotics biodegradation and metabolism	48	2 (4.2%)	2 (4.2%)
Translation	190	4 (2.1%)	16 (8.4%)
Folding, sorting, and degradation	53	2 (3.8%)	6 (11%)
Replication and repair	88	4 (4.5%)	0 (0%)
Membrane transport	243	13 (5.3%)	25 (10%)
Signal transduction	146	9 (6.2%)	14 (9.6%)
Cell motility	56	1 (1.8%)	4 (7.1%)
Drug resistance: Antimicrobial	61	3 (4.9%)	2 (3.3%)

In each cell, the number of genes assigned to the indicated KO category is indicated. When assigned using all genes, KO categories to which greater than 1000 or less than five genes were assigned were omitted in this table to avoid complexity. Note that some genes were assigned to multiple categories

<sup>a-c</sup>The percentage in parenthesis indicates the ratio between the number of genes assigned to each KO category for all genes and that for up- or downregulated genes (b/a or c/a % in each row)

**Table 3** Enriched KEGG pathways among up- and downregulated genes

KEGG pathway	Gene count	Count %	<i>p</i> value
Upregulated genes			
eco00730: thiamine metabolism	5	1.9	0.0011
eco00290: valine, leucine, and isoleucine biosynthesis	5	1.9	0.0035
eco01210: 2-oxocarboxylic acid metabolism	5	1.9	0.021
Downregulated genes			
eco00190: oxidative phosphorylation	22	9.0	$5.6 \times 10^{-12}$
eco01200: carbon metabolism	33	14	$6.6 \times 10^{-10}$
eco00010: glycolysis/gluconeogenesis	18	7.4	$2.6 \times 10^{-8}$
eco01120: microbial metabolism in diverse environments	43	18	$1.8 \times 10^{-8}$
eco01130: biosynthesis of antibiotics	36	15	$7.2 \times 10^{-5}$
eco00910: nitrogen metabolism	11	4.5	$6.8 \times 10^{-5}$
eco02060: phosphotransferase system (PTS)	12	4.9	0.0017
eco00020: citrate cycle (TCA cycle)	9	3.7	0.0021
eco00260: glycine, serine, and threonine metabolism	10	4.1	0.0053
eco03010: ribosome	16	6.5	0.0055
eco01110: biosynthesis of secondary metabolites	39	16	0.023
eco01230: biosynthesis of amino acids	19	7.8	0.027

The assigned enzyme commission (EC) number and KEGG pathway ID are shown in Supplementary Table S3, and the full data set is shown in Supplementary Table S4

in the nitrogen metabolism pathway, *glnA*, *narKGHJI*, *napAB*, *nirBD*, and *nrFA*, were downregulated (Table 3). These genes are all involved in nitrate reduction to ammonia and following glutamine synthesis, and thus, energy

acquisition is also limited at the nitrate respiration step. However, Venturelli et al. reported that 11 TCA cycle genes were upregulated between 2 and 8 min after the induction of MazF expression (Venturelli et al. 2017). The

difference in induction time (20 min in this study) might be the cause of these conflicting results.

### Enriched gene categories in DEGs

The result of the above GO enrichment analysis was inspected further on enriched gene categories. Regarding the upregulated genes (Table 4), the GO annotation cluster related to transposon function showed the highest enrichment score. Furthermore, we manually found that, out of 25 genes of the CP4-6 cryptic prophage, 10 genes were upregulated, whereas no gene was down-regulated. The CP4-6 prophage is in the middle of the segment I (from 262 to 296 kb) (Ferenci et al. 2009; Wang et al. 2010), and these 10 genes are part of the upregulated gene cluster (Fig. 1). Similarly, out of 30 genes of the Qin cryptic prophage, six and one genes were up- and down-regulated, respectively. The Qin prophage belongs to none of the segments I–III. These results again suggest activation of horizontally acquired and mobile genetic elements, following MazF activation.

The annotation cluster related to the fimbria/pilus function was found to be upregulated (Table 4). Type 1 fimbriae of *E. coli* facilitate attachment to biotic and abiotic surfaces (Blumer et al. 2005), and multiple TA systems including MazEF play important roles in biofilm formation through the regulation of fimbria production (Kim et al. 2009; Kolodkin-Gal et al. 2009). Therefore, this upregulation contributes to biofilm formation, which helps bacteria survive harsh conditions.

Regarding down-regulated genes (Table 5), the functional categories mentioned in Table 3 were again listed. In addition, the annotation cluster related to chaperon function was listed, and *groSL*, *dnaKJ*, *grpE*, *lsrR*, *hslUV*, *htpG*, *pykF*, *hslR*, *sodA*, *secB*, *hdeAB*, *ridA*, and *narJ* were included in this annotation cluster. The expression of some chaperone genes including *ibpAB*, *hslUV*, and *dnaKJ* is known to be induced upon deletion of the *mqsR* toxin-encoding gene or the overexpression of *mqsR* for 15 min (Kim et al. 2010). These facts and our results both suggest that some toxin proteins regulate the expression of chaperone network genes both negatively and positively. As *groSL*, *dnaKJ*, *grpE*, *hslUV*, *htpG*, and *hslR* are members of the  $\sigma^{32}$  (sigma factor 32)-regulon (Nonaka et al. 2006), these genes might be downregulated through  $\sigma^{32}$ . It should be noted that MazF might regulate the levels of chaperone-function genes directly and independently through its RNA interferase activity (see “Discussion” section for detail).

### Crosstalk of MazF to other TA systems

It is well known that activation of one TA system causes sequential or simultaneous activation of other TA system(s) and that free toxins (toxins unbound to cognate antitoxins) can enhance transcription from other TA operons (Kasari et al. 2013). Considering these facts, transcriptional regulation of other TA systems was inspected in our RNA-seq data.

Out of 37 known TA systems, expression of six toxin and one antitoxin genes was upregulated, while expression of two toxin and one antitoxin genes was downregulated

**Table 4** Enriched gene categories in upregulated genes

Category	Term	Gene count	Count %	<i>p</i> value
Annotation cluster 1, enrichment score: 4.3				
GOTERM_BP_DIRECT	GO:0015074~DNA integration	10	3.8	$4.9 \times 10^{-6}$
UP_KEYWORDS	Transposable element	15	5.6	$5.6 \times 10^{-6}$
UP_SEQ_FEATURE	chain: transposase insD for insertion element IS2A/D/F/H/I/K	6	2.3	$1.7 \times 10^{-5}$
Annotation cluster 2, enrichment score: 3.5				
UP_SEQ_FEATURE	chain: transposase insC for insertion element IS2A/D/F/H/I/K	6	2.3	$5.2 \times 10^{-6}$
UP_KEYWORDS	Transposable element	15	5.6	$5.6 \times 10^{-6}$
UP_KEYWORDS	Transposition	14	5.3	$2.4 \times 10^{-5}$
Annotation cluster 3, enrichment score: 3.3				
GOTERM_BP_DIRECT	GO:0009229~thiamine diphosphate biosynthetic process	6	2.3	$3.2 \times 10^{-4}$
UP_KEYWORDS	Thiamine biosynthesis	6	2.3	$3.2 \times 10^{-4}$
GOTERM_BP_DIRECT	GO:0009228~thiamine biosynthetic process	6	2.3	$5.2 \times 10^{-4}$
Annotation cluster 4, enrichment score: 2.6				
UP_KEYWORDS	Fimbrium biogenesis	10	3.8	$7.5 \times 10^{-6}$
UP_KEYWORDS	Transmembrane beta strand	11	4.1	$3.0 \times 10^{-4}$
GOTERM_BP_DIRECT	GO:0043711~pilus organization	7	2.6	$4.0 \times 10^{-4}$

Only the annotation clusters whose enrichment scores are above 2.5 are shown, and for each annotation cluster, only the categories showing three highest *p* values are listed. The full data set is shown in Supplementary Table S5

**Table 5** Enriched GO categories in downregulated genes

Category	Term	Gene count	Count %	<i>p</i> value
Annotation cluster 1, enrichment score: 7.1				
KEGG_PATHWAY	eco00190: oxidative phosphorylation	22	9.0	$5.6 \times 10^{-12}$
UP_KEYWORDS	Ubiquinone	11	4.5	$2.9 \times 10^{-10}$
GOTERM_CC_DIRECT	GO:0030964 ~NADH dehydrogenase complex	11	4.5	$2.8 \times 10^{-9}$
Annotation cluster 2, enrichment score: 6.8				
UP_KEYWORDS	Glycolysis	15	6.1	$3.0 \times 10^{-14}$
GOTERM_BP_DIRECT	GO:0006096 ~glycolytic process	15	6.1	$1.3 \times 10^{-12}$
KEGG_PATHWAY	eco01200: carbon metabolism	33	13	$6.6 \times 10^{-10}$
Annotation cluster 3, enrichment score: 4.3				
GOTERM_BP_DIRECT	GO:0042128 ~nitrate assimilation	10	4.1	$2.7 \times 10^{-6}$
UP_KEYWORDS	Nitrate assimilation	9	3.7	$4.9 \times 10^{-6}$
KEGG_PATHWAY	eco00910: nitrogen metabolism	11	4.5	$6.8 \times 10^{-5}$
Annotation cluster 4, enrichment score: 4.1				
UP_KEYWORDS	Ribosomal protein	16	6.5	$3.5 \times 10^{-7}$
UP_KEYWORDS	Ribonucleoprotein	16	6.5	$4.5 \times 10^{-7}$
GOTERM_MF_DIRECT	GO:0003735 ~structural constituent of ribosome	16	6.5	$1.8 \times 10^{-6}$
Annotation cluster 5, enrichment score: 3.4				
GOTERM_MF_DIRECT	GO:0051082 ~unfolded protein binding	8	3.3	$2.7 \times 10^{-6}$
GOTERM_BP_DIRECT	GO:0009408 ~response to heat	12	4.9	$5.6 \times 10^{-4}$
UP_KEYWORDS	Chaperone	11	4.9	0.0023
Annotation cluster 6, enrichment score: 3.1				
UP_KEYWORDS	Electron transport	19	7.8	$6.8 \times 10^{-6}$
GOTERM_BP_DIRECT	GO:0,009,061 ~anaerobic respiration	14	5.7	$4.2 \times 10^{-5}$
UP_KEYWORDS	Iron	27	11	$7.0 \times 10^{-4}$
Annotation cluster 7, enrichment score: 2.8				
UP_KEYWORDS	CF(1)	5	2.0	$5.3 \times 10^{-5}$
GOTERM_CC_DIRECT	GO:0045261 ~proton-transporting ATP synthase complex, catalytic core F(1)	5	2.0	$1.3 \times 10^{-4}$
GOTERM_MF_DIRECT	GO:0046961 ~proton-transporting ATPase activity, rotational mechanism	5	2.0	$9.9 \times 10^{-4}$

Only the annotation clusters whose enrichment scores are above 2.5 are shown, and for each annotation cluster, only the categories having three highest *p* values are shown. The full data set is shown in Supplementary Table S5

(Table 6). In these upregulated genes, two RNA interferase genes, *higB* and *yafO*, were included. Upregulation of *higB* (log<sub>2</sub>-fold change = 3.2, FDR =  $6.1 \times 10^{-3}$ ) did not accompany simultaneous upregulation of the cognate antitoxin gene, *higA* (log<sub>2</sub>-fold change = 1.4, FDR =  $2.9 \times 10^{-1}$ ), from which the ratio of toxin gene upregulation over antitoxin gene upregulation was calculated as 3.5. Upregulation of *yafO* (log<sub>2</sub>-fold change = 4.0, FDR =  $6.9 \times 10^{-4}$ ) accompanied elevated expression of cognate antitoxin gene *yafN* (log<sub>2</sub>-fold change = 2.5, FDR =  $3.3 \times 10^{-2}$ ; though this FDR value indicates insignificant upregulation), and similarly, the upregulation ratio was calculated as 2.8. Elevated expression of the other toxin gene, *yafQ*, was observed (log<sub>2</sub>-fold change = 2.3, FDR =  $4.5 \times 10^{-2}$ ; though this FDR value indicates insignificant upregulation) without simultaneous upregulation of cognate antitoxin gene *dinJ* (log<sub>2</sub>-fold change = 0.46, FDR =  $7.6 \times 10^{-1}$ ), and similarly, the

upregulation ratio was calculated as 3.6. Taken together, growth inhibition by *mazF* overexpression may be caused through cleavage of RNAs with multiple RNA interferases. Furthermore, it is clear that TA systems crosstalk at least partly.

## Discussion

Preceding studies have indicated that the primary role of MazF is cleaving bulk mRNA and inhibiting global translation (Zhang et al. 2003; Sauert et al. 2016). This hypothesis seems to be adequate, because only 175 of all 4318 *E. coli* genes (4.1%) do not contain ACA in their coding sequences (Table 1) (Venturelli et al. 2017). In contrast, RNA-seq analysis in this study indicated that MazF activation leads to biased regulation of RNA levels, which is independent of

**Table 6** Up- and down-regulated TA genes

Gene	log <sub>2</sub> -fold change	FDR	Toxin or antitoxin	Comments
Type II TA system, ribosome-independent RNA interferase				
<i>mazF</i>	5.8	$1.3 \times 10^{-6}$	Toxin	
Type II TA system, ribosome-dependent RNA interferase				
<i>yafO</i>	4.0	$6.9 \times 10^{-4}$	Toxin	
<i>higB</i>	3.2	$6.1 \times 10^{-3}$	Toxin	
Type II TA system, Inhibitors of cell division				
<i>yafW</i>	6.6	$4.6 \times 10^{-7}$	Antitoxin	Cognate toxin is YkfI
<i>ykfl</i>	5.7	$3.4 \times 10^{-6}$	Toxin	Cognate antitoxin is YafW
Type II TA system, inhibitor of phospholipid synthesis				
<i>gnsA</i>	- 4.1	$3.7 \times 10^{-4}$	Toxin	
Type I TA system				
<i>symE</i>	4.5	$3.4 \times 10^{-3}$	Toxin	
<i>ibsD</i>	- 3.5	$2.2 \times 10^{-3}$	Toxin	Neighboring gene to <i>sibE</i>
<i>sibE</i>	- 3.4	$5.2 \times 10^{-3}$	Antitoxin	Antitoxin RNA for <i>ibsE</i>
<i>ibsE</i>	- 4.4	$3.5 \times 10^{-4}$	Toxin	Repressed by <i>sibE</i> RNA
<i>hoka</i>	7.1	$1.9 \times 10^{-3}$	Toxin	

The full data set is shown in Supplementary Table S6

the presence and number of ACA sequences. Therefore, we conclude that MazF activation does not result in global and nonspecific translational inhibition and causes cells to shift to a specific cellular state. In agreement with this model, preceding studies have demonstrated that MazF activation leads to the selective synthesis of specific proteins (Amitai et al. 2009; Moll and Engelberg-Kulka 2012; Zorzini et al. 2016). It has also been demonstrated that not all ACA sequences in mRNAs are cleaved by MazF in vitro and in vivo (Tripathi et al. 2014), further supporting this model. Nevertheless, we do not exclude the possibility of global inhibition of translation by MazF, because in *mazF*-overexpressing cells, artificial ACA-free mRNAs are almost exclusively translated into proteins (Suzuki et al. 2006), and because MazF functions as an RNA interferase even in mammalian cells, mediating cellular mRNA degradation, inhibition of protein synthesis, and the induction of apoptosis (Shimazu et al. 2007).

An important question is how cellular levels of individual RNA species are adjusted following MazF activation. One possibility is modulation through RNA decay. As mentioned above, it seems that cleavage at ACA sequences occurs non-uniformly. Although the exact reason for this remains unclear, MazF seems to cleave at ACA sequences only within unstructured RNA regions, and those within structured regions are sterically hindered from cleavage (Zhang et al. 2004; Zhu et al. 2008; Vesper et al. 2011). The fate of cleaved RNA is still unclear, because 3'-ends of MazF-cleaved RNA are phosphate groups; RNAs cleaved by typical processing endonucleases such as RNases E/G bear 3'-hydroxyl groups, and RNases E/G are the primary endonucleases that trigger mRNA decay (Kushner 2002). Even so, one previous study proposed the possibility

that RNA cleaved by MazF is further degraded into four nucleotide monophosphates by RNases (Mok et al. 2015). Another study indicated that in response to stress, several RNA interferases might trigger mRNA decay as RNases E/G do (Deutscher 2006). Taken together, we propose a model, wherein following MazF activation, the cellular level of a specific RNA species is adjusted through the non-global cleavage of RNA at ACA sites and the further degradation of the cleaved RNA. However, we have shown here that MazF activation evokes the activation of other RNA interferases (Table 6), and thus, a more complicated cleavage and decay pathway must be considered.

Alternatively, RNA levels after MazF activation can be adjusted at the transcriptional level. However, the expression of all seven sigma factor genes was unchanged in this study (Supplementary Table S1). It should be noted that MazEF functions as a DNA-binding transcriptional repressor, and that MazE or the MazEF complex, alone or in conjunction, repress transcription from its own promoter (Marianovsky et al. 2001). Since, neither MazE nor the MazEF complex, alone or in conjunction, have been reported to regulate transcription from other promoters, we searched for the DNA-binding motif of the MazEF complex (gTATcTAcAATn-nanATTGATATATAC, where *n* is any nucleotide and capital letters denote important nucleotides) (Marianovsky et al. 2001) in the MG1655 chromosome. We failed to find highly homologous sequences except for the 5'-upstream region of the *mazEF* operon and found sequences showing low similarity in the 5'-upstream region of *mntP*, *yfgG*, and *tauA* (Supplementary Table S7). Among these three genes, only *mntP* was differentially expressed (log<sub>2</sub>-fold change = 3.1, FDR =  $8.4 \times 10^{-3}$ ). In addition, information



regarding promoters of upregulated genes in segments I and II were collected, but common features were not found (Supplementary Table S8). Collectively, we could find no obvious evidence of adjustment at the transcriptional level. Therefore, if RNA levels are adjusted at the transcriptional level, this modulation is presumably not governed by a single transcription factor, but rather a complex network.

Note that mechanisms of RNA modulation, both through RNA decay and at the transcriptional level can be compatible. Such mechanisms might work separately depending on the target genes. We believe that how cellular levels of individual RNA species are adjusted following MazF activation is an important target of future research. To unveil the function of MazEF, how indiscriminate cleavage of RNA and how specific adjustment of individual RNA species are associated should be addressed.

The finding that upregulated gene clusters are present in putative horizontally acquired DNA fragments (Fig. 1 and Supplementary Figs S2 and S3) is particularly interesting with respect to bacterial genome evolution. Many bacterial TA systems including *E. coli mazEF* are thought to enter the bacterial chromosome through horizontal gene transfer (Van Melderen and Saavedra De Bast 2009; Ramisetty and Santhosh 2016) and are frequently found on plasmids, prophages, transposons, and integrons (Bustamante et al. 2014; Mruk and Kobayashi 2014). In general, most horizontally transferred genes are lost from chromosomes just after this event (Kunin and Ouzounis 2003), because they are dispensable and metabolic burden is increased to replicate DNA (Cavalier-Smith 2005; Giovannoni et al. 2014). Nevertheless, portions of these elements can be retained on chromosomes, which can confer the ability to utilize specific nutrients or elevate tolerance to stresses. MazF might contribute to the maintenance of horizontally acquired genes by upregulating expression of such genes, so that cells can survive in harsh conditions. Under harsh conditions, MazF might stimulate adaptive evolution and generating phenotypic diversity. As mentioned above, the promoter sequences of upregulated genes in segments I and II have no common features (Supplementary Table S8), and crosstalk of TA systems are observed (Table 6). Therefore, we assume that the gene expression regulation in these segments is not governed by a single mechanism, but are co-ordinated and co-evolved each other.

In conclusion, both the validation (or expanded discovery) of already known facts and novel discoveries are described regarding the cellular role of MazF. The former includes (1) the selective synthesis of specific proteins, (2) alterations in chaperon networks, and (3) crosstalk between TA systems. The latter includes the fact that (1) the presence and number of ACA sequences is not related to cellular RNA levels, (2) upregulated gene clusters are present in putative horizontally acquired DNA fragments, (3) thiamine

and amino acid metabolism genes are specifically regulated, and (4) the energy acquisition pathway is limited at multiple steps.

**Acknowledgements** We would like to thank to the rest of iGEM team Tokyo\_Tech 2016 team members for collaboration on the early stages of this work. We are grateful to Ms. Tomoko Narisawa and Ms. Masako Sato for technical assistance. This work was supported by the Japan Society for the Promotion of Science (Grant number 17K07714).

## Compliance with ethical standards

**Conflict of interest** The authors declare no competing financial conflicts of interests.

## References

- Aakre CD, Phung TN, Huang D, Laub MT (2013) A bacterial toxin inhibits DNA replication elongation through a direct interaction with the  $\beta$  sliding clamp. *Mol Cell* 52:617–628
- Aiba H, Adhya S, de Crombrughe B (1981) Evidence for two functional gal promoters in intact *Escherichia coli* cells. *J Biol Chem* 256:11905–11910
- Amitai S, Kolodkin-Gal I, Hananya-Meltabashi M, Sacher A (2009) Engelberg-Kulka H (2009) *Escherichia coli* MazF leads to the simultaneous selective synthesis of both "death proteins" and "survival proteins". *PLoS Genet* 5:e1000390
- Blumer C, Kleefeld A, Lehnen D, Heintz M, Dobrindt U, Nagy G, Michaelis K, Emödy L, Polen T, Rachel R, Wendisch VF, Uden G (2005) Regulation of type 1 fimbriae synthesis and biofilm formation by the transcriptional regulator LrhA of *Escherichia coli*. *Microbiology* 151:3287–3298
- Bolger AM, Lohse M, Usadel B (2014) Trimmomatic: a flexible trimmer for Illumina sequence data. *Bioinformatics* 30:2114–2120
- Bustamante P, Tello M, Orellana O (2014) Toxin–antitoxin systems in the mobile genome of *Acidithiobacillus ferrooxidans*. *PLoS ONE* 9:e112226
- Cavalier-Smith T (2005) Economy, speed and size matter: evolutionary forces driving nuclear genome miniaturization and expansion. *Ann Bot* 95:147–175
- Culviner PH, Laub MT (2018) Global analysis of the *E. coli* toxin MazF reveals widespread cleavage of mRNA and the inhibition of rRNA maturation and ribosome biogenesis. *Mol Cell* 70:868–880
- Deutscher MP (2006) Degradation of RNA in bacteria: comparison of mRNA and stable RNA. *Nucleic Acids Res* 34:659–666
- Ellrott K, Yang C, Sladek FM, Jiang T (2002) Identifying transcription factor binding sites through Markov chain optimizations. *Bioinformatics* 18(Suppl 2):S100–S109
- Ferenci T, Zhou Z, Betteridge T, Ren Y, Liu Y, Feng L, Reeves PR, Wang L (2009) Genomic sequencing reveals regulatory mutations and recombinational events in the widely used MC4100 lineage of *Escherichia coli* K-12. *J Bacteriol* 191:4025–4029
- Giovannoni SJ, Thrash JC, Temperton B (2014) Implications of streamlining theory for microbial ecology. *ISME J* 8:1553–1565
- Huang DW, Sherman BT, Lempicki RA (2009) Systematic and integrative analysis of large gene lists using DAVID bioinformatics resources. *Nat Protoc* 4:44–57
- Kanehisa M, Goto S, Sato Y, Furumichi M, Tanabe M (2012) KEGG for integration and interpretation of large-scale molecular data sets. *Nucleic Acids Res* 40(Database issue):D109–D114

- Karcagi I, Draskovits G, Umenhoffer K, Fekete G, Kovács K, Méhi O, Balikó G, Szappanos B, Györfy Z, Fehér T, Bogos B, Blattner FR, Pál C, Pósfai G, Papp B (2016) Indispensability of horizontally transferred genes and its impact on bacterial genome streamlining. *Mol Biol Evol* 33:1257–1269
- Kasari V, Mets T, Tenson T, Kaldalu N (2013) Transcriptional cross-activation between toxin–antitoxin systems of *Escherichia coli*. *BMC Microbiol* 13:45
- Kim Y, Wang X, Ma Q, Zhang XS, Wood TK (2009) Toxin–antitoxin systems in *Escherichia coli* influence biofilm formation through YjgK (TabA) and fimbriae. *J Bacteriol* 191:1258–1267
- Kim Y, Wang X, Zhang XS, Grigoriu S, Page R, Peti W, Wood TK (2010) *Escherichia coli* toxin/antitoxin pair MqsR/MqsA regulate toxin CspD. *Environ Microbiol* 12:1105–1121
- Kolodkin-Gal I, Verdiger R, Shlosberg-Fedida A, Engelberg-Kulka H (2009) A differential effect of *E. coli* toxin–antitoxin systems on cell death in liquid media and biofilm formation. *PLoS ONE* 4:e6785
- Kunin V, Ouzounis CA (2003) The balance of driving forces during genome evolution in prokaryotes. *Genome Res* 13:1589–1594
- Kushner SR (2002) mRNA decay in *Escherichia coli* comes of age. *J Bacteriol* 184:4658–4665
- Magoc T, Wood D, Salzberg SL (2013) EDGE-pro: estimated degree of gene expression in prokaryotic genomes. *Evol Bioinform Online* 9:127–136
- Marianovsky I, Aizenman E, Engelberg-Kulka H, Glaser G (2001) The regulation of the *Escherichia coli* *mazEF* promoter involves an unusual alternating palindrome. *J Biol Chem* 276:5975–5984
- Masuda H, Tan Q, Awano N, Wu KP, Inouye M (2012) YeeU enhances the bundling of cytoskeletal polymers of MreB and FtsZ, antagonizing the CbtA (YeeV) toxicity in *Escherichia coli*. *Mol Microbiol* 84:979–989
- McCarthy JD, Chen Y, Smyth GK (2012) Differential expression analysis of multifactor RNA-seq experiments with respect to biological variation. *Nucleic Acids Res* 40:4288–4297
- Mets T, Kasvandik S, Saarma M, Maiväli Ü, Tenson T, Kaldalu N (2019) Fragmentation of *Escherichia coli* mRNA by MazF and MqsR. *Biochimie* 156:79–91
- Mok WW, Park JO, Rabinowitz JD, Brynildsen MP (2015) RNA futile cycling in model persisters derived from MazF accumulation. *mBio* 6:e01588-15
- Moll I, Engelberg-Kulka H (2012) Selective translation during stress in *Escherichia coli*. *Trends Biochem Sci* 37:493–498
- Mruk I, Kobayashi I (2014) To be or not to be: regulation of restriction–modification systems and other toxin–antitoxin systems. *Nucleic Acids Res* 42:70–86
- Nonaka G, Blankschien M, Herman C, Gross CA, Rhodius VA (2006) Regulon and promoter analysis of the *E. coli* heat-shock factor, sigma32, reveals a multifaceted cellular response to heat stress. *Genes Dev* 20:1776–1789
- Ramisetty BC, Santhosh RS (2016) Horizontal gene transfer of chromosomal Type II toxin–antitoxin systems of *Escherichia coli*. *FEMS Microbiol Lett* 363:fnv238
- Sauert M, Wolfinger MT, Vesper O, Müller C, Byrgazov K, Moll I (2016) The MazF-regulon: a toolbox for the post-transcriptional stress response in *Escherichia coli*. *Nucleic Acids Res* 44:6660–6675
- Shimazu T, Degenhardt K, Nur-E-Kamal A, Zhang J, Yoshida T, Zhang Y, Mathew R, White E, Inouye M (2007) NBK/BIK antagonizes MCL-1 and BCL-XL and activates BAK-mediated apoptosis in response to protein synthesis inhibition. *Genes Dev* 21:929–941
- Stothard P, Wishart DS (2005) Circular genome visualization and exploration using CGView. *Bioinformatics* 21:537–539
- Suzuki M, Roy R, Zheng H, Woychik N, Inouye M (2006) Bacterial bioreactors for high yield production of recombinant protein. *J Biol Chem* 281:37559–37565
- Tripathi A, Dewan PC, Siddique SA, Varadarajan R (2014) MazF-induced growth inhibition and persister generation in *Escherichia coli*. *J Biol Chem* 289:4191–4205
- Van Melderden L, Saavedra De Bast M (2009) Bacterial toxin–antitoxin systems: more than selfish entities? *PLoS Genet* 5:e1000437
- Venturelli OS, Tei M, Bauer S, Chan LJG, Petzold CJ, Arkin AP (2017) Programming mRNA decay to modulate synthetic circuit resource allocation. *Nat Commun* 8:15128
- Vesper O, Amitai S, Belitsky M, Byrgazov K, Kaberdina AC, Engelberg-Kulka H, Moll I (2011) Selective translation of leaderless mRNAs by specialized ribosomes generated by MazF in *Escherichia coli*. *Cell* 147:147–157
- Wang X, Kim Y, Ma Q, Hong SH, Pokusaeva K, Sturino JM, Wood TK (2010) Cryptic prophages help bacteria cope with adverse environments. *Nat Commun* 1:147
- Wang X, Lord DM, Cheng HY, Osbourne DO, Hong SH, Sanchez-Torres V, Quiroga C, Zheng K, Herrmann T, Peti W, Benedik MJ, Page R, Wood TK (2012) A new type V toxin–antitoxin system where mRNA for toxin GhoT is cleaved by antitoxin GhoS. *Nat Chem Biol* 8:855–861
- Yamaguchi Y, Inouye M (2011) Regulation of growth and death in *Escherichia coli* by toxin–antitoxin systems. *Nat Rev Microbiol* 19:779–790
- Yamazaki Y, Niki Y, Kato J (2008) Profiling of *Escherichia coli* chromosome database. *Methods Mol Biol* 416:385–389
- Zhang Y, Zhang J, Hoefflich KP, Ikura M, Qing G, Inouye M (2003) MazF cleaves cellular mRNAs specifically at ACA to block protein synthesis in *Escherichia coli*. *Mol Cell* 12:913–923
- Zhang J, Zhang Y, Zhu L, Suzuki M, Inouye M (2004) Interference of mRNA function by sequence-specific endoribonuclease PemK. *J Biol Chem* 279:20678–20684
- Zhu L, Phadtare S, Nariya H, Ouyang M, Husson RN, Inouye M (2008) The mRNA interferases, MazF-mt3 and MazF-mt7 from *Mycobacterium tuberculosis* target unique pentad sequences in single-stranded RNA. *Mol Microbiol* 69:559–569
- Zorzini V, Mernik A, Lah J, Sterckx YG, De Jonge N, Garcia-Pino A, De Greve H, Versées W, Loris R (2016) Substrate recognition and activity regulation of the *Escherichia coli* mRNA endonuclease MazF. *J Biol Chem* 291:10950–10960

**Publisher's Note** Springer Nature remains neutral with regard to jurisdictional claims in published maps and institutional affiliations.